Proceedings of the
44th IEEE Conference on Decision and Control, and
the European Control Conference 2005
Seville, Spain, December 12-15, 2005

Multivariable control for reference tracking on half car test rig

David Vaes, Kris Smolders, Jan Swevers and Paul Sas
K.U.Leuven, Department of Mechanical Engineering, Division PMA
B-3001 Heverlee, Belgium
david.vaes@mech.kuleuven.ac.be

***Abstract*— The multivariable tracking accuracy on an automotive vibration test rig can be improved by extending the current industrial off-line iterative feedforward procedure with a real time feedback controller. This paper compares two MIMO feedback controller design procedures in practice. First DK-iteration is used. This is the most common μ-synthesis method to design robust MIMO-controllers. Secondly a controller based on decoupling design is tested. This is a two step procedure. Step one is the calculation of a transformation of the inputs and the outputs to decouple the system as accurately as possible. Step two is the design of a decentralized controller (combination of independent SISO-controllers) for the transformed system. While the control design based on decoupling, using standard SISO $\mathcal{H}_\infty$ techniques is much simpler and more straightforward, the performance is comparable to that of the controller based on μ-synthesis.**

I. INTRODUCTION

During the design of a new car, vibration tests on a prototype or one of its components, using hydraulic test rigs, are important to adjust comfort and durability properties. For example, fig. 1(a) shows a four poster, where a car is placed on four hydraulic actuators. This is typically used for comfort analysis. Fig. 1(b) is a half axle test rig, used for durability tests, where the suspension can be loaded in vertical and horizontal direction. To make the vibration tests representative for the further life-time of the vehicle, reference signals (accelerations or forces) are measured during a test drive on a test track. These reference signals are reproduced on the test rig and often repeated until failure occurs.

(a) Four poster

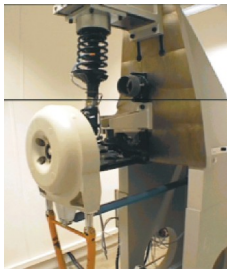

(b) Half axle test rig

Fig. 1. Examples of automotive vibration test rigs.

The calculation of the control signals for the actuators of the test rig, such that the measured signals on the test rig match the reference signals, is a MIMO tracking problem. Current industry practice to solve this tracking problem is the so-called *time waveform replication* (TWR) procedure. TWR is an off-line iterative process where the control-signals $\mathbf{u}(t)$ are updated based on the measured frequency response function matrix (FRF-matrix, $\mathbf{G^m}$) of the test rig and the tracking errors in the previous iteration [1]:

$$\mathbf{u^{(j+1)}}(t) = \mathbf{u^{(j)}}(t) + \alpha \left(\mathbf{G^m}\right)^{-1} \left(\mathbf{r}(t) - \mathbf{y^{(j)}}(t)\right), \qquad (1)$$

$\mathbf{r}(t)$ the reference signal, $\mathbf{y^{(j)}}(t)$ the output measured in iteration j and α a user-defined gain to guarantee convergence. When the model uncertainty is large, α must be small, yielding a slow convergence.

Due to the system nonlinearities, yielding large model uncertainties, a lot of iterations are required to obtain accurate tracking. As an indication, in industry, due to the long reference signals, about 1 week is needed to perform the complete TWR procedure. The number of iterations, can be reduced drastically by extending the current process with a high-performance feedback controller. [1] verifies this experimentally on a single-input-single-output (SISO) test rig. This paper considers the multiple-input-multiple-output (MIMO) case, and focusses on the controller design.

μ-synthesis is known as the optimal way to design robust MIMO-controllers. It is however a cumbersome procedure (section III-B). This paper compares, with respect to design complexity and obtained performance, μ-synthesis with a more straightforward controller design based on decoupling. The latter is a combination of two integrated steps: (1) the calculation of a decoupling transformation, optimized with respect to achievable control performance and (2) independent SISO-controllers designed for the diagonal elements of the transformed system. Experimental validation shows that both controllers obtain similar performance.

The paper is organized as follows: the next section describes the test rig used in this paper. Section III discusses the two different MIMO-control design methods. Both controllers are applied on the test rig in section IV, and it is shown that the number of iterations in the TWR procedure (1) is reduced from 12 to 3 by adding these controllers. Finally, section V draw some conclusions.

II. DESCRIPTION OF THE HALF CAR TEST RIG

The automotive test rig used in this paper, is a scale model of a half car test rig. A half car test rig contains a front or rear suspension of a car, which is excited by two hydraulic actuators. Typically, accelerations of the chassis are measured during a test drive and have to be reproduced on the test rig. Fig. 2 shows the scale model. The tires are represented by springs (k_{wr} and k_{wl}), which are connected to small

0-7803-9568-9/05/$20.00 ©2005 IEEE

masses representing the wheels. Between the wheels there is a flexible interconnection, corresponding with a anti-roll bar in a real suspension. The right and left suspension are represented by a spring (k_{sr} and k_{sl}) and a damper (c_{sr} and c_{sl}), and the car-body by the large upper mass (in black). This mass and the flexible interconnection between the wheels are centrally connected to the frame by rotational and linear bearings. The accelerations of the 'car body' are measured on the left and right corner of the upper mass. The test rig is excited by two hydraulic actuators at the bottom of the 'tires' (x_{wr} and x_{wl}). The actuators are position controlled by PID-controllers with a bandwidth of 30 Hz.

From a controller point of view this is a 2×2 system: the 2 inputs are the control signals for the actuators, the outputs are the right and left accelerations of the upper mass.

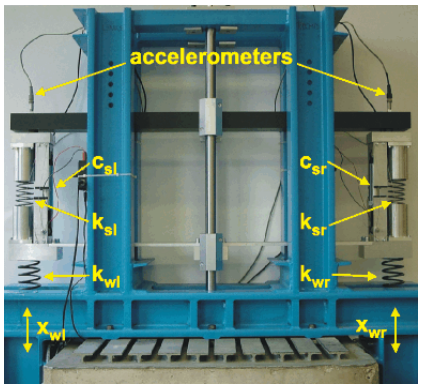

Fig. 2. Scale model of half car test rig.

The dampers are semi-active dampers. In this application, the control-signals to the dampers and hence the damping-values are kept constant. These dampers behave strongly nonlinear, yielding a nonlinear input-output behavior. Fig. 3(a) is the force - velocity characteristic of the damper for different settings. Fig. 3(b) shows the power spectral density (PSD) of the right acceleration for a sinusoidal input at 6 Hz on the right actuator. The higher harmonics in the response are caused by the nonlinearities in the damper.

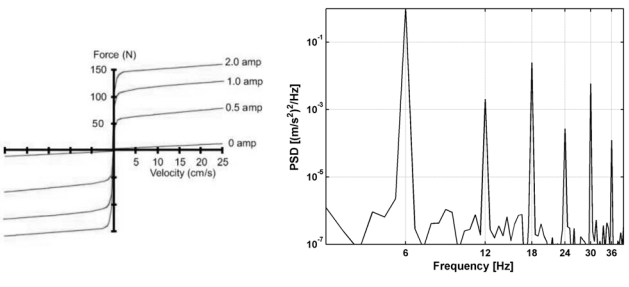

(a) (b)

Fig. 3. Nonlinear damper characteristic (a) and PSD of response to a sinusoidal input at 6 Hz (b).

The two dampers are also not identical due to production differences, yielding an asymmetrical test rig. This has important consequences for the decoupling procedure (see section III-C). A symmetrical test rig would result in a symmetrical FRF-matrix and identical diagonal elements. Fig. 4(a) and 4(b) show the two diagonal elements and the off-diagonal elements of the measured FRF-matrix respectively. The differences are clear. This FRF-matrix is estimated based on 5 minutes random excitation, using an H_1-estimator [2].

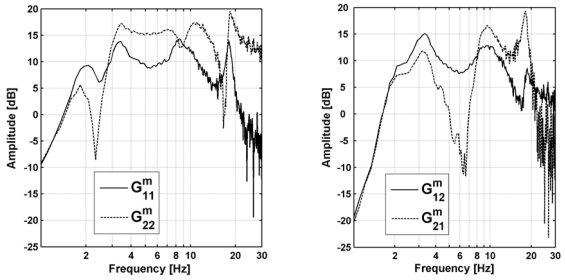

(a) (b)

Fig. 4. Amplitude of diagonal (a) and off-diagonal (b) elements of measured FRF-matrix $\mathbf{G^m}$ ($\mathbf{G^m_{ij}}$ represents the (i,j)-element of the measured FRF-matrix $\mathbf{G^m}$).

On real test rigs, the required tracking accuracy and the frequency band of interest are application dependent. The reference signals are measured during a test drive. On this scale-model, the bandwidth of the controller is made as large as possible (section III-A). The reference signals are generated on the test rig, by applying a typical road profile (uncorrelated noise with $1/s$-spectrum) to the test rig.

III. MIMO-CONTROLLER DESIGNS

This section compares two MIMO-controller designs: (1) a robust MIMO-controller, designed with μ-synthesis, and (2) a controller based on decoupling, designed as a combination of a decoupling transformation and independent SISO-controllers. The first is a complex design procedure, while the latter is simpler and more straightforward because it is based on standard SISO $\mathcal{H}_\infty$ design methods. The comparison will however show that, for the considered application, the performance of the two methods is comparable.

First, next subsection discusses shortly the design of a robustly stable SISO-controller and gives an indication of the maximal achievable bandwidth.

A. SISO robust controller design: $\mathcal{H}_\infty$ loopshaping

Many structures exist to represent the uncertainty of the nominal model. The uncertainty structure used in this paper is the *multiplicative output uncertainty*, because it leads to the simplest expressions for robust stability. It is also the most widespread structure used to represent complex uncertainty of MIMO systems [3]. This structure supposes that the real system is unknown, but in the set:

$$(1 + W_o \Delta_o)\, G \qquad |\Delta_o| < 1, \tag{2}$$

with G the nominal model and W_o the multiplicative uncertainty. A SISO-controller is robustly stable (stable for all systems within the uncertainty set) if [3]:

$$|T(j\omega)| < 1/|W_o(j\omega)| \qquad \forall \omega, \tag{3}$$

with T the complementary sensitivity. To estimate W_o in practice, FRFs are measured at five different excitation levels. Due to system nonlinearities, the FRFs depend on the excitation levels. The differences between different excitation levels are incorporated in W_o to guarantee stability of the controller for the range of excitation levels relevant for the TWR procedure.

Fig. 5 shows the inverse of an estimate of the multiplicative uncertainties W_o^{-1} on the diagonal elements of the FRF-matrix in full and dashed line. It is clear that, to satisfy (3), $|T|$ must roll off around 15 Hz.

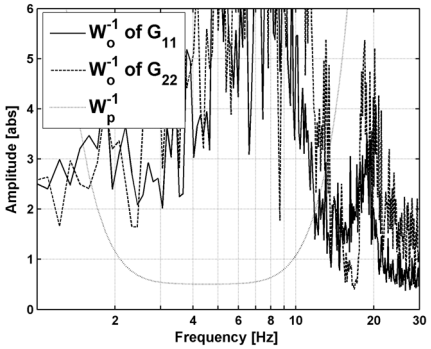

Fig. 5. Inverse of the multiplicative uncertainty of diagonal elements of the FRF-matrix (full and dashed line), and the inverse of the performance weight W_p (dotted line).

Accurate tracking is obtained in the frequency band where the sensitivity S is small. Because T has to be small around 15 Hz, a reasonable estimate of the maximal bandwidth of S is 10 Hz. The measured accelerations are negligible below 2 Hz, hence, S does not have to be small below 2 Hz. These specifications correspond to the following requirement:

$$|S(j\omega)| < 1/|W_p(j\omega)| \quad \forall\omega, \tag{4}$$

with W_p^{-1} as shown in fig. 5.

A SISO-controller which satisfying (3) and (4) is then designed using $\mathcal{H}_\infty$ mixed-sensitivity loopshaping. SISO $\mathcal{H}_\infty$ mixed-sensitivity loopshaping calculates a controller C based on the convex minimization of [3]:

$$\left\| \begin{bmatrix} W_p S \\ \bar{W}_o T \end{bmatrix} \right\|_\infty = \sup_\omega \left(\sqrt{|W_p S|^2 + |\bar{W}_o T|^2} \right), \tag{5}$$

with $\bar{W}_o$ a low order approximation of the estimated multiplicative uncertainty W_o, of which the inverse is shown in fig. 5. When the minimum is smaller than 1, the controller is robustly stable (3) and has nominal performance (4).

B. MIMO robust controller design: μ-synthesis

MIMO-performance is measured by the MIMO weighted sensitivity $\|\mathbf{W_p S}\|_\infty$. The performance specifications for both accelerometers are the same, hence, $\mathbf{W_p}$ is chosen as a diagonal matrix: $\mathbf{W_p} = W_p \mathbf{I}$, with W_p as shown in fig. 5.

Direct identification of a MIMO-model $\mathbf{G}(s)$ based on the measured FRF-matrix, using non-linear least squares [2] or subspace identification [4] methods, failed to produce an accurate stable model. Therefor an indirect approach is used. A SISO-model is fitted on each element of the FRF-matrix independently, and then combined into a MIMO-model, yielding a 42nd order model.

For the MIMO-case (2) generalizes to:

$$(\mathbf{I} + \mathbf{W_o \Delta_o})\,\mathbf{G} \qquad \|\mathbf{\Delta_o}\|_\infty < 1. \tag{6}$$

The estimation of $\mathbf{W_o}$ is, analogue to the SISO-case, based on FRF-matrices measured at different excitation levels.

The full line in fig. 6 is the estimation of the MIMO multiplicative uncertainty based on FRF-matrices measured at 5 different excitation levels. The dashed line shows the low order approximation $\bar{\mathbf{W}}_\mathbf{o}(s)$ as it is used in the controller synthesis. Better fits can be obtained with higher order models, but that is not advisable because (i) the estimation of the uncertainty is not exact, so a more accurate approximation makes no sense, and (ii) this complicates the controller synthesis and yields unnecessary high order controllers.

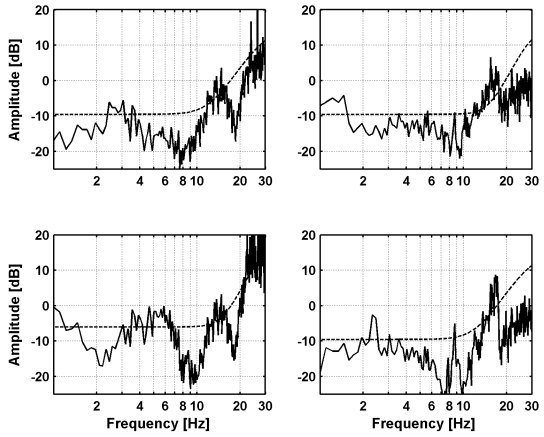

Fig. 6. Estimation of MIMO-uncertainty based on 5 measured FRF-matrices (full line) and low order approximation $\bar{\mathbf{W}}_\mathbf{o}$ (dashed line).

Fig. 7 shows the scheme to analyze robust stability of the closed loop system. The control scheme of fig. 7 is robustly stable if and only if [3]:

$$\mu_{\mathbf{\Delta_o}}\left(\mathbf{W_o}(j\omega)\mathbf{T}(j\omega)\right) < 1 \quad \forall\omega, \tag{7}$$

with $\mu_{\mathbf{\Delta_o}}$ the structured singular value, calculated with respect to the structure of $\mathbf{\Delta_o}$, which is diagonal.

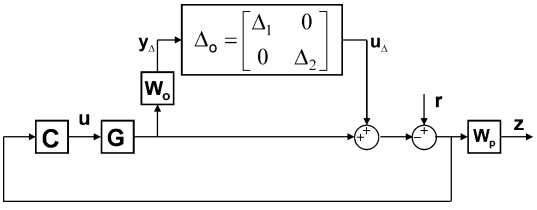

Fig. 7. General control scheme to analyze MIMO robust stability and performance with μ-analysis.

No controller synthesis method exist to design a controller satisfying (7). Replacing the μ-norm by the ∞-norm (and

using MIMO $\mathcal{H}_\infty$ loopshaping) is however very conservative. A less conservative upper bound on the μ-norm, can be calculated with the following convex minimization:

$$\mu_{\mathbf{\Delta}}(\mathbf{M}) \leq \min_{\mathbf{D}\in\mathcal{D}} \bar{\sigma}(\mathbf{DMD}^{-1}), \tag{8}$$

with $\mathcal{D}$ the set of all matrices which commute with $\mathbf{\Delta}$.

This leads to the best known μ-synthesis method, namely DK-iteration, where in each iteration first an $\mathcal{H}_\infty$-controller is synthesized for the scaled problem (the K-step) and than the $\mathbf{D}$-scalings are optimized (the D-step). Both steps are convex optimizations, but joint convexity is not guaranteed, yielding conservatism in the controller. Moreover, the true μ-optimal controller is generally of infinite order, so finite-order, sub-optimal, approximations have to be used.

The DK-iteration using $\bar{\mathbf{W}}_\mathbf{o}$ of fig. 6 and $\mathbf{W_p} = W_p\mathbf{I}$ with W_p as specified in fig. 5 results in a 66th order controller. To apply it in real-time, the order is reduced to 35, using optimal Hankel norm approximation [5].

The combination of the cumbersome identification, the unavoidable conservatism in the design, the complex DK-iteration design and the resulting high order controller (requiring model reduction to be applicable in real-time) makes the μ-synthesis a difficult task in practice.

C. Design of controller based on decoupling

Fig. 8 shows the basic idea behind the controller design based on decoupling. First, the inputs $\mathbf{u}$ and outputs $\mathbf{y}$ of the systems are transformed by the matrices $\mathbf{T_u}$ and $\mathbf{T_y}$, such that the relation between the transformed inputs $\mathbf{u_T} = \mathbf{T_u^{-1}u}$ and transformed outputs $\mathbf{y_T} = \mathbf{T_y y}$ is as diagonal as possible. Secondly, SISO-controllers are designed for the diagonal elements of the transformed system $\mathbf{G_d}$:

$$\mathbf{G_d} = \mathbf{T_y G T_u}. \tag{9}$$

The combination of the independent SISO-controllers is called the *decentralized controller*. Perfect decoupling, hence $\mathbf{G_d}$ perfectly diagonal, is only obtained for symmetrical systems. In general, $\mathbf{T_u}$ and $\mathbf{T_y}$ are the result of an optimization procedure which decouple $\mathbf{G_d}$ as accurately as possible.

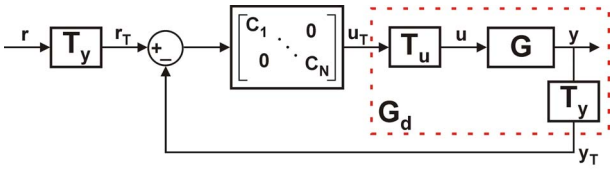

Fig. 8. Basic control scheme of a controller based on decoupling.

Robust stability of all independent SISO-controllers does not guarantee stability of the whole decentralized controller. [6] shows that a decentralized controller, designed for $\mathbf{G_d^m} = \mathbf{T_y G^m T_u}$, with $\mathbf{G^m}$ the measured FRF-matrix of the system, is stable if for each SISO-control loop:

$$|T_i^m(j\omega)| < \mu_{C_d}^{-1}(\mathbf{E^m}(j\omega)) \qquad \forall\omega, i \tag{10}$$

with T_i^m the complementary sensitivity based on the measured FRF of the i'th SISO-loop and the μ-norm calculated with respect to the structure of the controller, which is diagonal. $\mathbf{E^m}$ a measure for the interaction in $\mathbf{G_d^m}$:

$$\mathbf{E^m} = \left(\mathbf{G_d^m} - \mathbf{D_d^m}\right)\left(\mathbf{D_d^m}\right)^{-1}, \tag{11}$$

with $\mathbf{D_d^m} = diag\{\mathbf{G_d^m}_{ii}\}$ ($diag\{\ldots\}$ denotes the diagonal matrix consisting of the elements between braces).

Because MIMO robust controller design is cumbersome, many methods have been developed to determine $\mathbf{T_u}$ and $\mathbf{T_y}$. The easiest-to-use decoupling methods are based on matrix-decompositions. [7] introduces the *commutative controller*, based on the eigenvalue decomposition. [8] launched a controller based on the singular value decomposition.

These methods have however some serious drawbacks. First of all, these methods are based on the FRF-matrix at one or two frequencies, yielding accurate decoupling only in a limited bandwidth around these frequencies. Secondly, when using singular or eigenvalue decompositions, the degrees of freedom in $\mathbf{T_u}$ and $\mathbf{T_y}$ are inherently limited. For example in the eigenvalue decomposition the left and right transformation matrices are the inverse of each other. And thirdly the decoupling procedure is not integrated with the subsequent decentralized control design.

Remark that the goal of the decoupling transformations $\mathbf{T_u}$ and $\mathbf{T_y}$ is to maximize the achievable performance of the decentralized controller. That's why a different approach is followed in this paper: a decoupling transformation is considered optimal when it maximizes the upper bound in (10). This corresponds to the following optimization:

$$\min_{\mathbf{T_u},\mathbf{T_y}} \left\{ \sup_{\omega} \left[\mu_{C_d}(\mathbf{E^m}(j\omega))W(j\omega)\right] \right\}, \tag{12}$$

with $W(j\omega)$ a frequency dependent weighting function, to emphasize the frequency band of interest. $\mathbf{E^m}(j\omega)$ is a function of $\mathbf{T_u}$ and $\mathbf{T_y}$ (11). Remark that $\mathbf{T_u}$ and $\mathbf{T_y}$ are calculated based on the measured FRF-matrix, and that no MIMO-identification is required.

This is a non-convex optimization, requiring accurate starting values. The starting values can be obtained by one of the existing methods [7], [8] or by *modal decoupling*. In modal decoupling, the transformation matrices are:

$$\mathbf{T_u} = \begin{bmatrix} 1 & 1 \\ -1 & 1 \end{bmatrix}, \ \mathbf{T_y} = \begin{bmatrix} -\frac{1}{2} & \frac{1}{2} \\ \frac{1}{2} & \frac{1}{2} \end{bmatrix}. \tag{13}$$

These matrices transform the real inputs and outputs into *rotational* and *translational* inputs and outputs. For a symmetrical test rig, they would perfectly decouple the system. However, due to the asymmetry in the system (section II) this modal decoupling is not optimal, but can be used as starting value for the optimization routine.

Fig. 9 shows the obtained upper bounds in (10). The dotted line shows that a decentralized controller for the original system (without using decoupling), must have low performance ($|T| < 0.4$) around 2.3 Hz to guarantee stability. When modal decoupling (13) is used (dashed line), the complementary sensitivity must drop off around 10 Hz to guarantee stability. This would seriously limit the frequency range where accurate tracking can be achieved. Finally, the

full line shows that, for optimized transformation matrices (12) the upper bound is larger than 1 up to 16 Hz. Remark that this constraint on T is comparable to the constraint due to the model uncertainty, shown in fig. 5. Hence, accurate decoupling up to higher frequencies is not required.

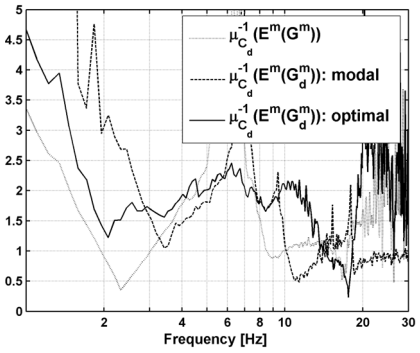

Fig. 9. Upper bounds of (10) for the measured FRF $\mathbf{G^m}$ (dotted line), the decoupled FRF $\mathbf{G^m_d}$ using modal decoupling (dashed line) and using optimized decoupling (full line).

Two independent robust SISO-controllers, satisfying (10) are now designed using the techniques discussed in section III-A. The uncertainty used to check robust stability (3) is the uncertainty on the diagonal elements of $\mathbf{G^m_d}$.

The performance of both feedback controllers is compared using the ∞-norm of the weighted sensitivity (section III-B): $\|\mathbf{W_p S}\|_\infty = \sup_\omega(\bar{\sigma}(\mathbf{W_p S}))$. The full line in fig. 10 is $\bar{\sigma}(\mathbf{W_p S})$ for the controller based on μ-synthesis. The sensitivity is calculated using the measured FRF-matrix. The dotted line shows $\bar{\sigma}(\mathbf{W_p S})$ for the controller based on decoupling supposing perfect decoupling, hence, neglecting the off-diagonal elements in $\mathbf{G^d_m}$. This shows that the designed performance is almost the same as the performance of the controller based on μ-synthesis. The performance of the controller based on decoupling applied on the complete FRF-matrix is shown in the dashed line. The performance slightly deteriorates due to the neglected interaction. The controller design based on decoupling is however much simpler because no MIMO-identification, μ-synthesis and control model reduction are required.

IV. EXPERIMENTAL VALIDATION ON TEST RIG

Both controllers are now applied to the test rig. In a first test, a feedforward signal $\mathbf{u_{ff}^{(1)}}$ is calculated based on the inverse of the measured FRF-matrix:

$$\mathbf{u_{ff}^{(1)}} = (\mathbf{G^m})^{-1}\,\mathbf{r}. \tag{14}$$

This feedforward is then combined with the feedback controllers designed in the previous section, as shown in fig. 11. This scheme allows to calculate the feedforward based on the open-loop system, yielding that the same TWR procedure can be used with and without feedback.

Fig. 12 and 13 show the tracking results on the test rig. The bold line is the PSD of the reference signal. The dotted line is the PSD of the tracking error when only the feedforward

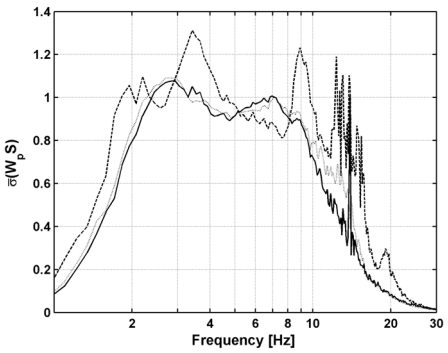

Fig. 10. $\bar{\sigma}(\mathbf{W_p S})$ based on the measured FRF-matrix: for the controller designed with μ-synthesis (full line), for the controller based on decoupling, supposing perfect decoupling (dotted line) and for the controller based on decoupling applied on the complete FRF-matrix (dashed line).

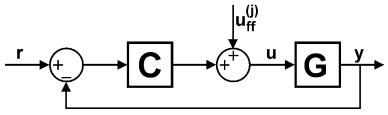

Fig. 11. Combination of TWR procedure and feedback controller.

(14) is applied. The thin full line and the dashed line show the PSD of the tracking error when this feedforward is combined with the controller based on decoupling and on μ-synthesis respectively. It is clear that the tracking error is reduced significantly by adding the feedback controller. The performance of both feedback controllers is comparable.

One might expect, based on fig. 10, that between 3 and 4 Hz the controller based on μ-synthesis yields a smaller tracking error than the controller based on decoupling. Fig. 12 and 13 show, however, the opposite effect. This can be explained as follows. The maximal singular value of the weighted sensitivity in fig. 10 is a measure for the worst case tracking error [3]. In fact, the following inequalities apply:

$$\underline{\sigma}(\mathbf{S}) \leq \|\mathbf{e}\|_2/\|\mathbf{r}\|_2 \leq \bar{\sigma}(\mathbf{S}), \tag{15}$$

with $\mathbf{e}$ and $\mathbf{r}$ the tracking errors and reference signals respectively. The considered reference signals are not uncorrelated random signals, but generated on the test rig. Between 3 and 4 Hz, the direction of the reference signals is close to the direction of the singular vector, corresponding to the smallest singular value of the sensitivity for the controller based on decoupling, yielding a smaller tracking error than predicted by $\bar{\sigma}(\mathbf{S})$.

Finally, the complete TWR procedure (1) is performed on the test rig. To guarantee convergence, α in (1) has to be set to 0.7. Fig. 14 and 15 show the evolution of the RMS of the tracking error during all iterations of the TWR procedure for the right and left accelerometer respectively. Without feedback, 12 iterations are required before the TWR procedure has converged. With any of the two feedback controllers, and $\alpha = 0.7$, the tracking errors are smaller after three iterations than without feedback after 12 iterations. The tracking is only slightly improved by a fourth iteration. These input-signals can now be used in durability or comfort analysis tests.

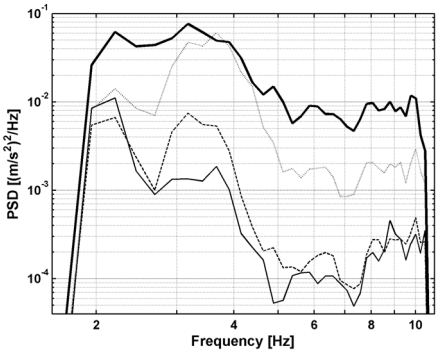

Fig. 12. PSDs of reference signal (bold line) and tracking errors using (1) only feedforward (dotted line), (2) feedforward feedback based on decoupling (full line) and (3) feedforward and feedback based on μ-synthesis (dashed line) for the right accelerometer.

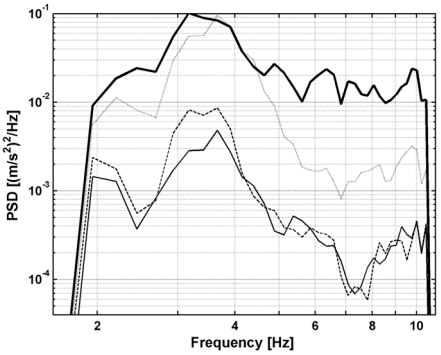

Fig. 13. PSDs of reference signal (bold line) and tracking errors using (1) only feedforward (dotted line), (2) feedforward feedback based on decoupling (full line) and (3) feedforward and feedback based on μ-synthesis (dashed line) for the left accelerometer.

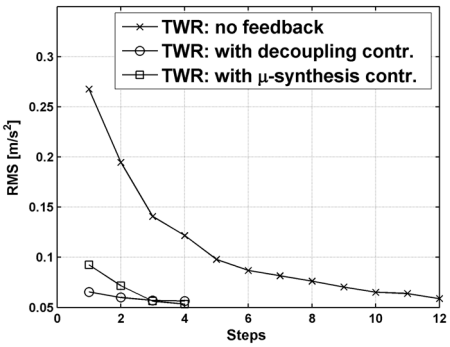

Fig. 14. RMS of right tracking error during all iterations of TWR procedure: without feedback ($\times$), with controller based on decoupling (o) and with controller based on μ-synthesis ($\square$).

Two important conclusions can be drawn from these experiments: (1) the number of iterations is reduced drastically by adding a feedback controller to the TWR procedure and (2) the simple decoupling controller yields similar performance as the complex μ-synthesis controller.

V. CONCLUSIONS

This paper compares experimentally two MIMO-control design methods with respect to the design complexity and the obtained performance. The considered application is an automotive vibration test rig tracking problem.

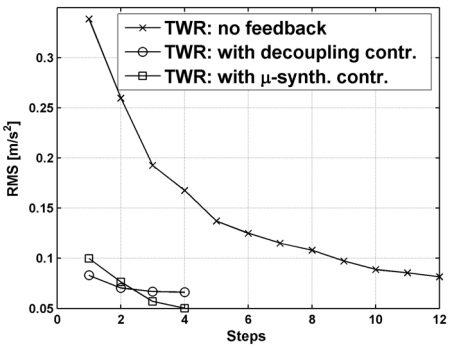

Fig. 15. RMS of left tracking error during all iterations of TWR procedure: without feedback ($\times$), with controller based on decoupling (o) and with controller based on μ-synthesis ($\square$).

Firstly, a robust controller is designed using μ-synthesis, yielding the following problems: cumbersome MIMO-identification, conservatism in the design and a high order controller. Secondly, a controller based on decoupling is designed. This design consists of two integrated steps: (1) the calculation of the transformation matrices and (2) the design of independent SISO-controllers for the diagonal elements of the transformed system. Straightforward SISO $\mathcal{H}_\infty$-techniques can be used to design the controllers. The performance of both controllers is comparable. Adding these MIMO feedback controllers to the industrial off-line iterative feedforward procedure reduces the number of iterations from 12 to 3.

ACKNOWLEDGEMENTS

This research is sponsored by the Belgian programme on Interuniversity Poles of Attraction, initiated by the Belgian State, Prime Minister's Office, Science Policy Programming (IUAP). D. Vaes is a Research Assistant of the Fund for Scientific Research (F.W.O.) - Flanders (Belgium). The scientific responsibility remains with its authors.

REFERENCES

[1] J. De Cuyper, M. Verhaegen, J. Swevers, "Off-line Feed-forward and $\mathcal{H}_\infty$ Feedback Control for improved Tracking on an industrial vibration test rig", *Control Engineering Practice*, 11, 2003, pp. 129-140.

[2] R. Pintelon, J. Schoukens, *System Identification: A Frequency Domain Approach*, IEEE Press, New York (NY, USA), 2001.

[3] S. Skogestad, I. Postlethwaite, *Multivariable Feedback Control, Analysis and Design*, John Wiley & Sons, New York (NY, USA), 1996.

[4] P. Van Overschee, B. De Moor, "Continuous-time frequency domain subspace system identification", *Signal Processing*, 52, 1996, pp. 179-194.

[5] K. Glover, "All Optimal Hankel Norm Approximation of Linear Multivariable Systems, and Their $\mathcal{L}_\infty$-error Bounds", *International Journal of Control*, 39 (6), 1984, pp. 1115-1193.

[6] S. Skogestad, M. Morari, "Robust Performance of Decentralized Control Systems by Independent Designs", *Automatica*, 25 (1), 1989, pp. 119-125.

[7] A. G. J. MacFarlane, "Commutative controller: A new technique for the design of multivariable control systems", *Electronic letters*, 6, 1970, pp. 121-123.

[8] Y. S. Hung, A. G. J. MacFarlane, *Multivariable feedback: A quasi-classical approach*, Springer-Verlag, New York (NY, USA), 1982.